Progress In Electromagnetics Research, PIER 62, 107–125, 2006

ELLIPTICALLY BENT SLOTTED WAVEGUIDE CONFORMAL FOCUSED ARRAY FOR HYPERTHERMIA TREATMENT OF TUMORS IN CURVED REGION OF HUMAN BODY

R. C. Gupta and S. P. Singh

Department of Electronics Engineering
Institute of Technology
Banaras Hindu University
Varanasi-221 005, U.P., India

Abstract—In present paper, a novel and effective hyperthermia applicator utilizing an elliptically bent conformal array of longitudinal slots in narrow wall of rectangular waveguide is analyzed by two different approaches, *viz.*, the vector potential method and Fresnel-Kirchhoff scalar diffraction field theory. The agreement between two theories is reasonably very good. This configuration is mainly intended as a specialized and very effective applicator for hyperthermia treatment of tumor within curved portions of human body such as abdomen, neck, chest *etc.* Each slot of the conformal array is excited by a coaxial line probe. It is proposed that the interior of the waveguide be filled with water to provide a good impedance match with the bio-medium. The contour distribution of specific absorption rate (SAR) in x-z plane, SAR distribution in y-direction and parameters such as penetration depth, power absorption coefficient, effective field size (EFS) due to the conformal array as well as single slot are evaluated and compared at 433 MHz. The results for contour SAR distribution at 433 MHz for elliptically bent conformal array are also compared with those for other array configurations such as circularly bent conformal array and planar array. The effect of change in phase and amplitude excitation of each slot of the array on SAR distribution is also examined. The results demonstrate that slotted waveguide conformal array offers marked improvement in SAR distribution and penetration depth over single slot. It also has better focusing ability as compared with planar array for controlled amplitude and phase excitations of the elements.

1. INTRODUCTION

The design of microwave array applicator for hyperthermia treatment of tumor within curved portion of human body such as abdomen, neck, chest *etc.* is motivated by the need to elevate the temperature throughout the tumor to the therapeutic temperature range (43° to 50°C) and selectively heat deep-seated tumors while sparing normal tissue. The design of an effective hyperthermia applicator to transfer microwave energy to the treatment area is an important problem. The applicator must possess focusing ability, be light in weight, compact and compatible to the shape of heating region of the body. The applicator should also have the ability to modify absorbed power distributions during use by changing the amplitude and phase of individual applicators. These requirements, put together provide a challenging list of specifications that demand innovation in applicator design beyond known conventional array configurations. Microwave hyperthermia is one of the important tools in the therapeutic and non-invasive treatment of tumors in human body [1]. The precise focusing of beam is still challenging, and the conformal antenna array is a prospective solution to this problem, owing to the flexible contour of the array geometry, which can blend with the local body surface area and its potential to steer the beam in the desired direction. An elliptical array is a real conformal applicator which conforms to the shape of the treatment area of the human body, such as abdomen, neck, chest *etc.* Conformal arrays are useful for scanning over a wide range of angles, typically $> \pm 70°$, whereas conventional planar arrays have substantial gain reductions and mismatch losses over wide scan angles.

A number of studies on array configurations using different types of applicators for hyperthermia treatment of cancer have been reported in the literature [2–10], such as linear array [2, 3], planar array [4], hexagonal array [5], circular/ring array [6, 7], cylindrical array [8], spherical array [9], annular phased array [10] and many other array configurations using waveguides, horns *etc.*

In the present paper, a novel microwave hyperthermia conformal array system, which differs somewhat from the above conventional array applicators, is reported. The technique is based on a elliptically bent conformal array of longitudinal slots in narrow wall of water-loaded rectangular waveguide, which is a realistic hyperthermia array and is compatible with the curved surface of human body such as abdomen, neck, chest *etc.* The use of slots in waveguide has proved to be a promising means of launching high frequency radiation in bio-media. The longitudinal slots in narrow wall of rectangular waveguide are commonly called edge slots, which possess the key advantages of relative ease of construction, higher radiation efficiency, higher-power handling capability, and broader frequency bandwidth over the broad-wall slots. The unique characteristic feature of this new type of array is its compatibility with the treatment surface and its focusing ability. The slotted waveguide conformal array is loaded with water to match its impedance with heating medium and hence sufficient energy deposition at the tumor site can be achieved. Also, loading the array applicator with water reduces the dimensions of the slots making them suitable for array configuration. Elliptically bent slotted waveguide conformal array offers the advantage of being lightweight, rugged, compact and easy to handle. The specific absorption rate (SAR), which is the rate at which microwave energy is absorbed per unit mass of biological tissue has been used by hyperthermia researchers to characterize energy deposition and heating patterns in tissues and in biological models. The expression for specific absorption rate (SAR) as a function of space co-ordinates is derived for the conformal array in direct contact with a heating medium (muscle/tumor). The present analysis is based on two different approaches, namely the vector potential method [11] and Fresnel-Kirchhoff scalar diffraction field theory [12]. The expressions for electric field and the results for SAR in the heating medium obtained by two methods agree well with each other. The penetration depth (PD_h) is defined as depth where SAR value is down to 13.5 percent of the maximum in the heating medium. Power absorption coefficient (PAC_h) is obtained by taking the inverse of penetration depth in heating medium. The effective field size (EFS) is the area covered by 50% (-3 dB) SAR contour [10]. The contour of SAR distributions, penetration depth, power absorption coefficient and effective field size are evaluated for the array and single slot at 433 MHz, one of the ISM frequencies. Each slot of the conformal array is excited by a coaxial line probe. The effect of phase and amplitude control of excitation for individual slots of the array on SAR distributions has been theoretically analyzed at a frequency of 433 MHz. The contour SAR distributions at 433 MHz for elliptically bent conformal array are also compared with those for circularly bent conformal array and planar array and it is shown that the elliptically bent conformal array has better focusing ability as compared with planar array for controlled amplitude and phase excitations of the elements.

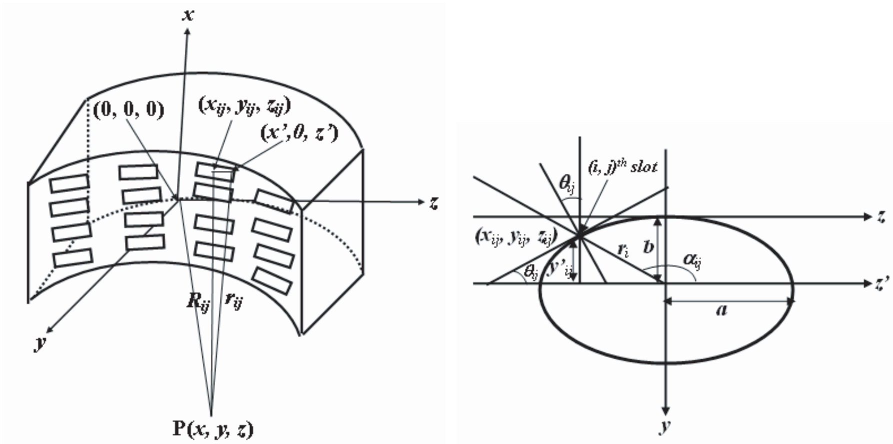

(a) (b)

Figure 1. (a) Elliptically bent conformal array of longitudinal slots in narrow wall of water-loaded rectangular waveguide (b) angular position and angular orientation of (i, j)th slot of the conformal array.

2. ANALYSIS OF ELLIPTICALLY BENT SLOTTED WAVEGUIDE CONFORMAL ARRAY

An elliptically bent conformal array of longitudinal slots in narrow wall of water-loaded rectangular waveguide terminated in heating-medium (muscle/tumor) is schematically illustrated in Fig. 1(a) and the orientation of an element of the array is shown in Fig. 1(b). For slotted waveguide conformal array, slot radiates into one hemisphere only. The heating-medium has complex permittivity of $\varepsilon_h^* = \varepsilon - j\varepsilon'$. L and w are the length and width of each slot respectively. In present analysis, heating-medium is considered to be extending upto infinity along positive y-direction and each slot aperture is assumed to be in direct contact with the heating surface. In an array environment, the element pattern is affected by the mutual coupling between the elements. This effect is generally considered to be secondary and is neglected in this study, since experimentally it is investigated that coupling between adjacent waveguide elements is on the order of -30 dB, presumably low due to high medium losses [4]. Let centre of (i, j)th slot (*i.e.*, ith slot in an elliptical arc subarray and jth subarray) in the conformal array is situated at the point (x_{ij}, y_{ij}, z_{ij}) and the coordinates of field point P be (x, y, z). Assume the coordinates of a point in the aperture of (i, j)th slot with the centre of that slot acting as the origin to be $(x', 0, z')$. All the antenna sub-arrays considered in this study are assumed to have rotational symmetry and conformal array consists of elliptical arc subarrays stacked vertically (*i.e.*, in x-direction). The electric-field in heating medium due to the (i, j)th slot of the conformal array can be found by following two different approaches: the vector potential method and Fresnel-Kirchhoff scalar diffraction field theory.

2.1. The Vector Potential Method

In this technique, a longitudinal slot is considered to be equivalent to a magnetic dipole radiator as discussed by Wolff [11]. According to the equivalence principle, the magnetic surface current density at (i, j)th infinitesimal slot is given by

$$\overline{M}_s = -\hat{n}_{ij} \times \overline{E}_s = -(\hat{y}\cos\theta_{ij} + \hat{z}\sin\theta_{ij}) \times E_{sx}\hat{x} \tag{1}$$

where $\hat{x}$ is a unit vector in the direction of x-axis and $\hat{n}_{ij}$ is a unit vector in the direction perpendicular to the aperture of (i, j)th slot. θ_{ij} is the orientation of the longitudinal axis of (i, j)th slot of the conformal array measured from positive z'-axis. The electric vector potential, $\overline{F}_s$ can be found as

$$\begin{aligned} \overline{F}_s &= \frac{\varepsilon}{4\pi}\int_{-w/2}^{w/2}\int_{-L/2}^{L/2} \frac{\overline{M}_s e^{-jkr_{ij}}}{r_{ij}} dz'dx' \\ &= \frac{\varepsilon \overline{E}_{sx} wLe^{-jkr_{ij}}}{4\pi r_{ij}}(-\hat{y}\sin\theta_{ij} + \hat{z}\cos\theta_{ij}) \end{aligned} \tag{2}$$

where k is the complex propagation constant in heating medium $(= \omega\sqrt{\mu_0\varepsilon(1 - j\sigma_h/\omega\varepsilon)})$, ω is the angular frequency of the operating microwave. $\sigma_h(= \omega\varepsilon')$ and ε' are conductivity and imaginary part of permittivity of the heating-medium respectively. For infinitesimal slot $r_{ij} \approx R_{ij}$.

The near electric field can computed from the relation

$$\overline{E} = -j\omega\overline{A} - \frac{j\omega}{k^2}\nabla(\nabla\cdot\overline{A}) - \frac{1}{\varepsilon}\nabla\times\overline{F} \tag{3}$$

where $\overline{A}$ is magnetic vector potential. In the present case $\overline{A} = 0$. It is noted from the symmetry of the slot that there is no variation of the field in the x-direction, i.e., $\partial/\partial x = 0$. The near electric field for infinitesimal slot can be obtained from Eqns. (2) and (3). If the slot is long with sinusoidal field distribution, it is subdivided into a number of infinitesimal slots of length $\Delta z'$. As the number of subdivisions is increased, each infinitesimal slot approaches a length dz'. The electric field $[E_s(z)]$ across each infinitesimal slot is assumed constant. The near field of long slot is therefore a superposition of the fields of each of the small segments. The near electric field due to the small element dz' can be put in the following form

$$dE_x = \frac{E_s(z)e^{-jkr_{ij}}}{4\pi r_{ij}^2}\left(jk+\frac{1}{r_{ij}}\right)[(y-y_{ij})\cdot\cos\theta_{ij}+(z-z_{ij}-z')\cdot\sin\theta_{ij}]dz'dx' \tag{4}$$

Total near field due to (i,j)th long slot at the field point (x,y,z) is therefore

$$\begin{aligned} E_{ij}(P) \;=\; & \int_{-w/2}^{w/2}\int_{-L/2}^{L/2}\frac{E_l(z)e^{-jkr_{ij}}}{4\pi r_{ij}^2}\left(jk+\frac{1}{r_{ij}}\right) \\ & [(y-y_{ij})\cdot\cos\theta_{ij}+(z-z_{ij}-z')\cdot\sin\theta_{ij}]dx'dz' \end{aligned} \tag{5}$$

where $E_l(z)$ is sinusoidal electric field distribution across the aperture of long slot [13] in narrow wall of rectangular waveguide for TE_{10} mode given by

$$E_l(z) = E_m \sin k_h\left(\frac{L}{2}-|z'|\right) \tag{6}$$

where E_m is the maximum electric field intensity in the slot.

2.2. Fresnel-Kirchhoff Scalar Diffraction Field Theory

The electric-field in heating medium due to the (i,j)th slot of the conformal array can be found by Fresnel-Kirchhoff scalar diffraction formula [12] given below.

$$E_{ij}(P) = \frac{1}{4\pi}\int_{area} E_l(z)\frac{e^{-jkr_{ij}}}{r_{ij}}\left[\left(jk+\frac{1}{r_{ij}}\right)\hat{n}_{ij}\cdot\hat{r}_{ij}+jk\hat{n}_{ij}\cdot\hat{s}_{ij}\right]dx'dz' \tag{7}$$

where $i = 1,2,\ldots,4$ and $j = 1,2,\ldots,4$, $\hat{r}_{ij}$ is the unit vector along r_{ij} from source point to the field point, $\hat{s}_{ij}$ is the unit vector normal to the wavefront at the aperture of (i,j)th slot. For nearly all aperture illuminations that concentrate energy along the normal to aperture of (i,j)th slot, $\hat{n}_{ij}\cdot\hat{s}_{ij}$ may be taken to be zero, since $\hat{n}_{ij}$ is almost perpendicular to $\hat{s}_{ij}$.

Since

$$\vec{r}_{ij} \;=\; \{x-(x_{ij}+x')\}\cdot\hat{x}+(y-y_{ij})\cdot\hat{y}+\{z-(z_{ij}+z')\}\cdot\hat{z} \tag{8}$$

$$\hat{r}_{ij} \;=\; \frac{\vec{r}_{ij}}{r_{ij}} \tag{9}$$

Therefore,

$$\hat{n}_{ij} \cdot \hat{r}_{ij} = \frac{(y - y_{ij}) \cdot \cos\theta_{ij} + (z - z_{ij} - z') \cdot \sin\theta_{ij}}{r_{ij}} \tag{10}$$

After substituting for the term $\hat{n}_{ij} \cdot \hat{r}_{ij}$ of the integrand of Eqn. (7) from Eqn. (10), the electric field at point $P(x, y, z)$ due to (i, j)th slot can be put in simplified form as given in Eqn. (5).

2.3. Position of (i, j)th Slot of the Conformal Array

The length of each slot may be taken as $L = \lambda_d/2$, where λ_d is the wavelength in water. The width w of the slot can be chosen from the relation $2w \ll \lambda_d$ and is taken as $\lambda_d/20$. The spacing between any two adjacent slots from center to center in x-direction can be selected using the relation $d = w + \Delta d$, where Δd can be adjusted for proper separation between slots. The y_{ij} and z_{ij} co-ordinates of each slot can be calculated from the following relations

$$y_{ij} = b - r_i \sin\alpha_i \tag{11}$$

and

$$z_{ij} = r_i \cos\alpha_i \tag{12}$$

where $r_i = \frac{ab}{\sqrt{b^2\cos^2\alpha_i + a^2\sin^2\alpha_i}}$, $2a$ and $2b$ are the major and minor axes of ellipse of the arc array respectively. α_{ij} is the angular position of the ith element of jth subarray from z'-axis. α_{ij} can be found by

$$\alpha_{ij} = \alpha_n - \Delta\alpha \times (n - i) \tag{13}$$

where $i = 1, 2, \ldots, n$, n is number of elements in jth subarray (in the present case $n = 4$) and $\Delta\alpha$ can be chosen using the relation $\Delta\alpha \geq 2\tan^{-1}\left(\frac{L}{2a}\right)$ so that any two adjacent slots have proper separation. There is uniform angular distribution of the elements on the elliptical arc. The angular position of the last/nth element of jth subarray, α_n can be found by

$$\alpha_n = \frac{180° + \Delta\alpha}{2} + \left(\frac{n}{2} - 1\right) \cdot \Delta\alpha. \tag{14}$$

2.4. Orientation of (i, j)th Slot of Elliptical Conformal Array

The orientation of (i, j)th slot is defined by an angle θ_{ij}, which is the angle between z'-axis and tangent to the elliptical arc drawn at the angular position of (i, j)th slot. For any elliptical arc subarray (keeping x_{ij} constant)

$$\left(\frac{y_{ij}}{b}\right)^2 + \left(\frac{z_{ij}}{a}\right)^2 = 1 \tag{15}$$

By geometry, it can found that θ_{ij} is equal to the slope of tangent drawn on point (x_{ij}, y_{ij}, z_{ij}) of the ellipse defined by Eqn. (15).

Thus

$$\theta_{ij} = \tan^{-1}\left(-\frac{b^2}{a^2}\frac{z_{ij}}{(b - y_{ij})}\right) \tag{16}$$

2.5. Total Near Electric Field and SAR Value Due to Conformal Phased Array

The total electric field of the array at a near-field point $P(x, y, z)$ can be obtained by superposition. The total electric field E_t at the observation point $P(x, y, z)$ due to entire array [2] is given by

$$E_t(P) = \sum_j \sum_i W_{ij} E_{ij}(P) \tag{17}$$

where

$$\begin{aligned} W_{ij} &= |W_{ij}| e^{j\delta_{ij}} \\ &= \text{weighting factor for } (i, j)\text{th slot of the arc array} \end{aligned} \tag{18}$$

If we want to focus the energy at point F, the electric field due to all elements of the array at point F should be in same phase. If phase excitation (phase weighing factor) of each element of the array is managed to be negative of the phase of the field that is produced at point F by same element operating coherently, the fields due to all elements of the array at point F will be added in phase. Thus, microwave energy is focused at point F. In order to focus the array field at a point F we must have phase excitation of the (i, j)th slot equal to

$$\delta_{ij} = (-1)\{\text{phase of } \overline{E}_{ij}(F)\} \tag{19}$$

When Eqn. (19) is used in Eqn. (17), all the terms in the summation are added in phase at point F and not at other observation points because fields at other observation points will not be in phase at all.

The amplitude excitations (amplitude weighting factors) of the elements of the array are controlled according to requirement of effective size of heating and location of heating, e.g., for heating the bio-medium in the middle region of the aperture of the array, the amplitude weighting factors of inner elements of the array can be kept equal to 1 and those of outer elements are kept less than 1 to get desired heating pattern. The size of SAR distribution at tumor location (at focused point) can be controlled by appropriate amplitude and phase excitations of each slot of the array. This can be done as follows: power from a source is divided into as many equal parts as there are slots in the array using a power divider. Each of the output ports of the power divider is to be connected to the coaxial probe/loop through variable attenuator and phase-shifter for exciting the slot. Adjustment of magnitude and phase of weighting factor can be done by appropriately changing the variable attenuator and phase-shifter respectively connected in the path of signal for each slot of the array.

The specific absorption rate (SAR) in heating-medium can be evaluated by

$$SAR = \frac{\sigma_h |E_t(P)|^2}{2\rho_h} \tag{20}$$

where ρ_h is density of the heating-medium.

2.6. Design of of Elliptically Bent Slotted Waveguide Conformal Array

Water-loaded rectangular waveguide EIA WR-229 with $5.8 \times 2.9\,\mathrm{cm}^2$ aperture size is chosen for slotted conformal array operating at 433 MHz. The permittivity of water is taken to be $78 - j1.25$ [14]. Total 16 slots are taken for conformal array with 4 slots ($n = 4$) on each of the four elliptical arc subarrays. The computed dimensions of each slot are $L = 3.9\,\mathrm{cm}$ and $w = 0.4\,\mathrm{cm}$. Practical values of $2a = 30\,\mathrm{cm}$ and $2b = 18\,\mathrm{cm}$ for abdomen region of human body are taken in present computation. Here angular separation between two subsequent slots, $\Delta\alpha$ and centre to centre spacing between any two adjacent slots in x-direction (d) are taken equal to 25° and 3 mm respectively. The four slots are situated at 52.5°, 77.5°, 102.5° and 127.5° from z'-axis on each four subarrays.

2.7. Numerical Results and Discussion

The properties of tumor are assumed to be identical to muscle in the present numerical solution. The complex permittivity [15] and density [16] of heating-medium (muscle/tumor) are taken to be $\varepsilon_h^* = 47 - j34.9$ and $\rho_h = 1050\,\mathrm{Kg/m}^3$ respectively in the present computation. The contour of SAR distribution in heating-medium (muscle/tumor region) for elliptically bent conformal array of longitudinal slots in narrow wall of water-loaded rectangular waveguide are quantified theoretically at 433 MHz utilizing both the approaches, *viz.*, the vector potential method and Fresnel-Kirchhoff scalar diffraction field theory using MATLAB® and the results are presented in Figs. 2–5.

Fig. 2 illustrates the contour of relative SAR distribution (in dB) for elliptically bent coherent/unfocused conformal array in x-z plane at 433 MHz. The SAR values are normalized to the maximum value of SAR in heating-medium. The effective field size (EFS) is also evaluated and the results are presented in Table 1.

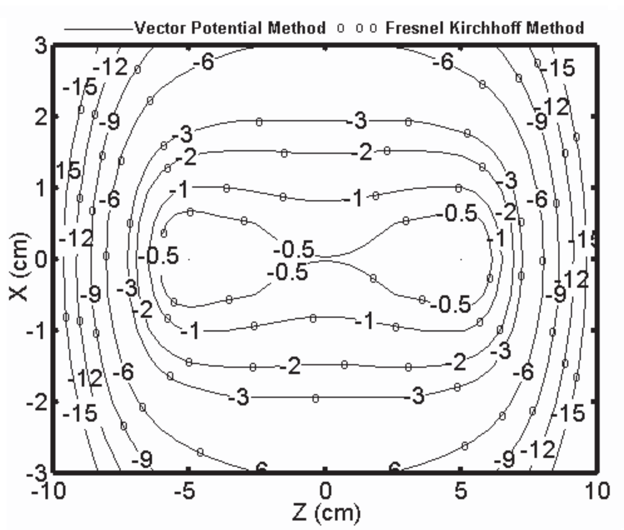

Figure 2. Relative SAR contour (in dB) in x-z plane at $y = 3.5\,\mathrm{cm}$ for elliptically bent conformal coherent array.

Fig. 3 shows the relative SAR contour (in dB) focused [2] at the point (0 cm, 3.5 cm, $z = 2\,\mathrm{cm}$) by calculating phase due to each slot of the array with the help of Eqn. (19) for elliptically bent conformal array. In this case, amplitude excitation of each slot of the array is kept uniform. Two heating spots for focused array with appropriate phase excitation of each slot are obtained with EFS equal to 13 and $0.9\,\mathrm{cm}^2$ in comparison to single heating spot obtained for coherent/unfocused conformal array (EFS $= 41\,\mathrm{cm}^2$) (Table 1). The larger hot spot ($13\,\mathrm{cm}^2$) is focused at the expected point (0 cm, 3.5 cm, $z = 2\,\mathrm{cm}$). By comparing the focused SAR-distribution contour with unfocused/coherent SAR contour given in Fig. 2, it is concluded that by changing the phase of each slot, the hot spot can be steered to the desired location/point to treat deep-seated tumors.

Table 1. Parameters of array and single slot at 433 MHz.

Parameters	Elliptically bent conformal array	Circularly bent conformal array	Planar array	Single slot
PD_h	4.20 cm	4.20 cm	4.20 cm	0.90 cm
PAC_h	23.80 m^{-1}	23.80 m^{-1}	23.80 m^{-1}	110.98 m^{-1}
EFS uniform phase and amplitude excitation (w_{ij}=1, δ_{ij}=0)	41 cm^2	41 cm^2	41cm^2	11cm^2
EFS different phase excitation (w_{ij}=1, δ_{ij} from Equation 19)	13 cm^2 0.9cm^2	10 cm^2	9cm^2	-
EFS different amplitude excitation (w_{ij} from Table 2, δ_{ij}=0)	34 cm^2	30cm^2	26cm^2	-
EFS different phase and amplitude excitation (w_{ij} from Table 2, δ_{ij} from Equation 19)	12 cm^2	11cm^2	15cm^2	-

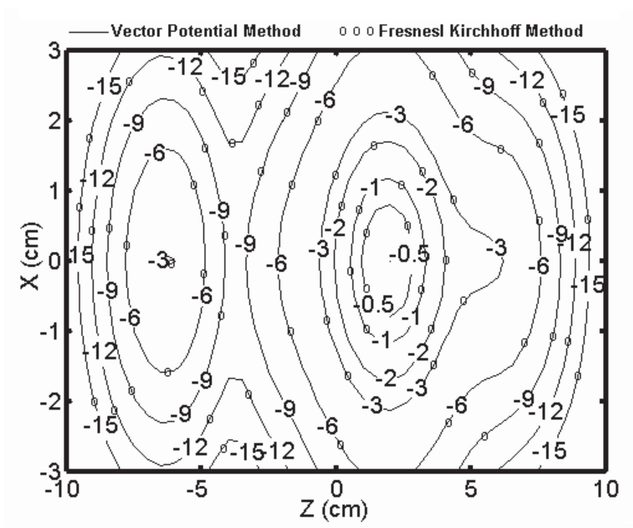

Figure 3. Relative SAR contour (in dB) in x-z plane at $y = 3.5$ cm for elliptically bent conformal phased array with different phase excitation of each slot.

Table 2. Profile of amplitude excitation of (i, j)th slot of the conformal array.

i j	1	2	3	4
1	0.7	1	1	0.7
2	0.7	1	1	0.7
3	0.7	1	1	0.7
4	0.7	1	1	0.7

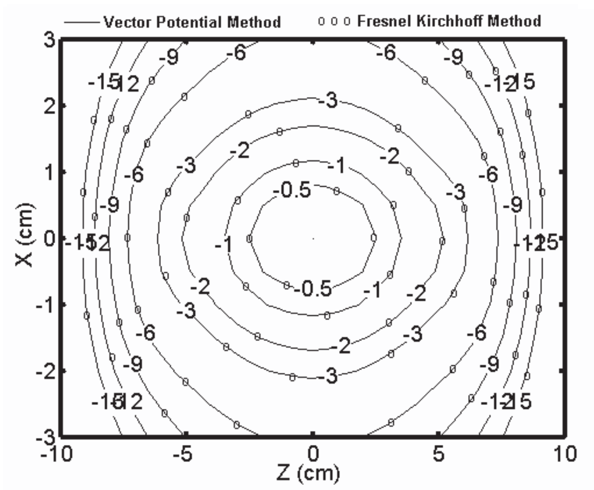

Figure 4. Relative SAR contour (in dB) in x-z plane at $y = 3.5$ cm for elliptically bent conformal array with different amplitude excitation of each slot.

Fig. 4 depicts the relative SAR contour (in dB) in x-z plane for the profile of amplitude excitation, given in Table 2 for each slot of the conformal array. Here phase excitation of each slot of the array is kept constant to observe the effect of amplitude excitation of each slot on the SAR distribution. The effective field size (EFS) is $34\,\text{cm}^2$ in this case, while EFS is $41\,\text{cm}^2$ for coherent conformal array (Table 1). Thus, the size of heating spot can be optimized by proper amplitude excitation for each slot of the conformal array.

In Fig. 5, the relative SAR contour (in dB) in x-z plane is shown for the profile of amplitude excitation given in Table 2 for each slot of the conformal array and for the phase calculated for each slot of the conformal array with the help of Eqn. (19) to focus energy at the

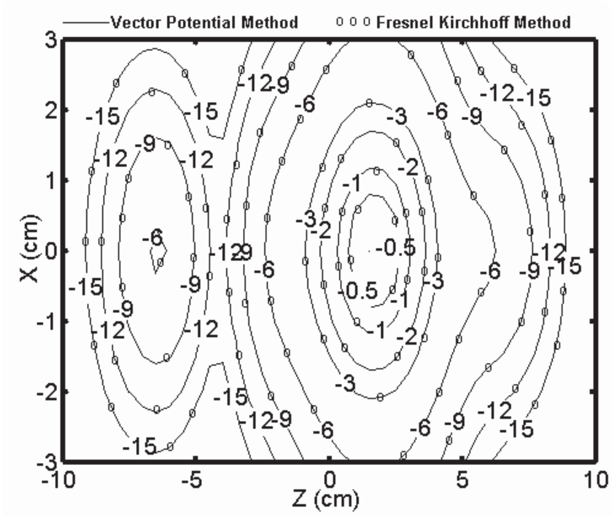

Figure 5. Relative SAR contour (in dB) in x-z plane at $y = 3.5\,\mathrm{cm}$ for elliptically bent conformal phased array with different phase and amplitude excitations of each slot.

point (0 cm, 3.5 cm, $z = 2\,\mathrm{cm}$). Now, EFS is $12\,\mathrm{cm}^2$, whereas EFS is $41\,\mathrm{cm}^2$ for coherent conformal array (Table 1). Therefore, desired shape (EFS) of SAR distribution at tumor location (at focused point) can be obtained by appropriate amplitude and phase excitations of each slot of the conformal array.

The SAR distributions are computed utilizing the vector potential method/Fresnel-Kirchhoff scalar diffraction field theory for elliptically and circularly bent conformal arrays and planar array and the results are presented in Figs. 6–10. The centre of each slot in circularly bent conformal array has same (x, y, z) position as the respective slot in elliptically bent conformal array. The diameter of circularly bent conformal array is taken to be 30 cm ($= 2a$). Each slot in planar array has same x and z coordinates as the respective slot in elliptically bent conformal array. The y-coordinate of each slot in planar array is taken to be zero. Remaining specifications for circularly bent conformal array and planar array are the same as for elliptically bent conformal array.

Normalized SAR distributions along y-direction for elliptically and circularly bent conformal arrays, planar array and single slot have been compared in Figure 6. The penetration depth ($\mathrm{PD_h}$) and power absorption coefficient ($\mathrm{PAC_h}$) in heating medium for the arrays and single slot are presented in Table 1. It can be seen from Fig. 6

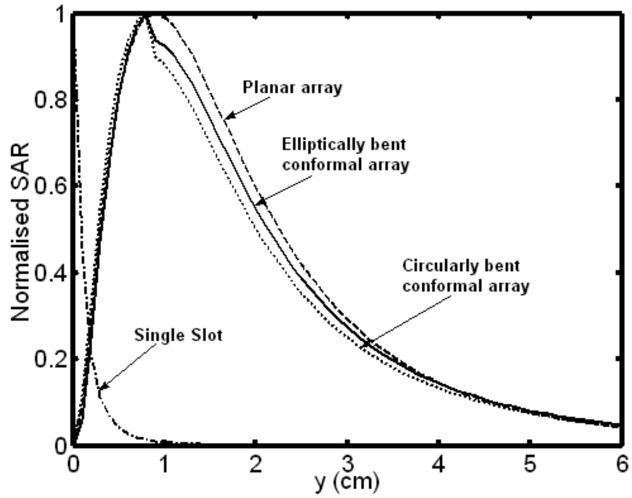

Figure 6. Normalized SAR distribution in y-direction at $x = z = 0\,\text{cm}$ for coherent arrays and single slot.

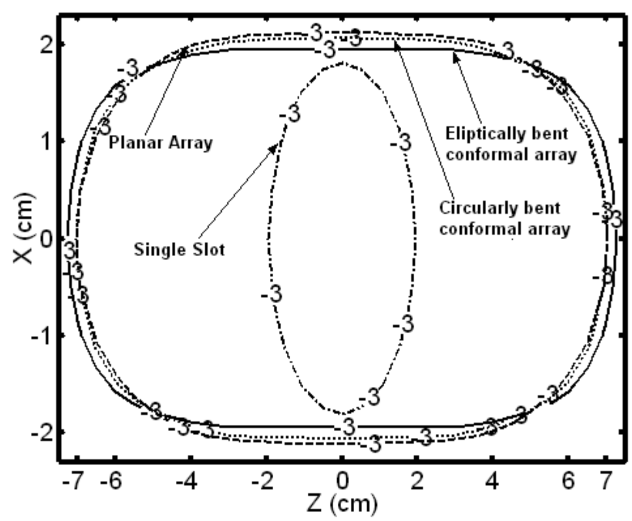

Figure 7. $-3\,\text{dB}$ SAR contour in x-z plane at $y = 3.5\,\text{cm}$ for coherent arrays.

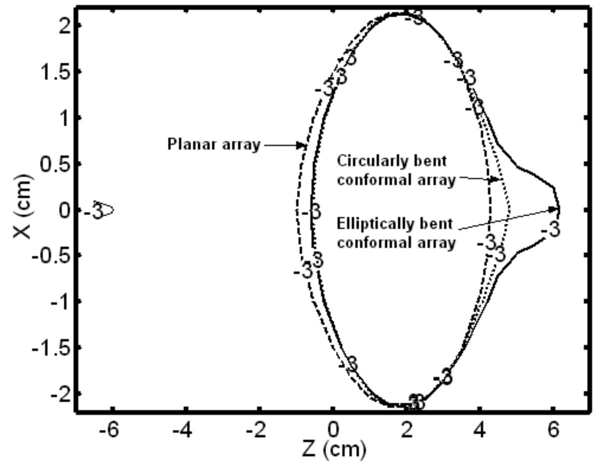

Figure 8. -3 dB SAR contour in x-z plane at $y = 3.5$ cm for phased arrays with different phase excitation of each slot.

and Table 1 that elliptically bent conformal array can heat tumors at greater depth in comparison to the single slot applicator. Also all the arrays considered have the same penetration depth.

The -3 dB contour (effective field/heating size) of relative SAR distribution (in dB) for coherent/unfocused elliptically and circularly bent conformal arrays, planar coherent array and single slot are compared in x-z plane at 433 MHz (Fig. 7). The effective field size (EFS) evaluated for coherent arrays and single slot are listed in Table 1. From Fig. 7 and Table 1, it can be inferred that slotted array applicator can heat much larger area in transverse direction than single slot. All coherent arrays have almost equal EFS. The elliptically bent conformal array provides slightly greater energy spread along z-direction while other type of arrays give slightly better energy spread along x-direction.

Fig. 8 shows the -3 dB contour SAR distribution (in dB) focused [2] at the point (0 cm, 3.5 cm, $z = 2$ cm) for elliptically and circularly bent conformal phased arrays and planar array. In this case, amplitude excitation of each slot of array under study is kept uniform. For the elliptically bent conformal phased array larger EFS is steered at the expected point (0 cm, 3.5, $z = 2$ cm) (Table 1) as compared with circularly bent conformal array and planar array.

In Fig. 9, the -3 dB contour SAR distribution (in dB) in x-z plane is shown for the profile of amplitude excitation, given in Table 2 for each slot of the array for elliptically and circularly bent conformal phased arrays and planar array. Here phase excitation of each slot of the

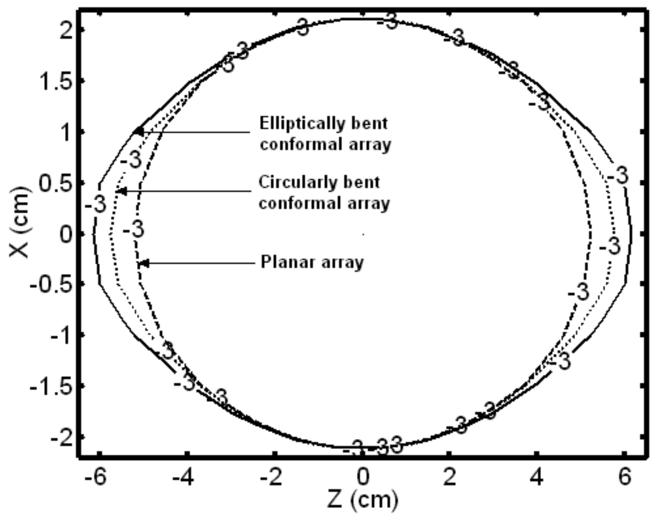

Figure 9. $-3\,\text{dB}$ SAR contour in x-z plane at $y = 3.5\,\text{cm}$ for arrays with different amplitude excitation of each slot.

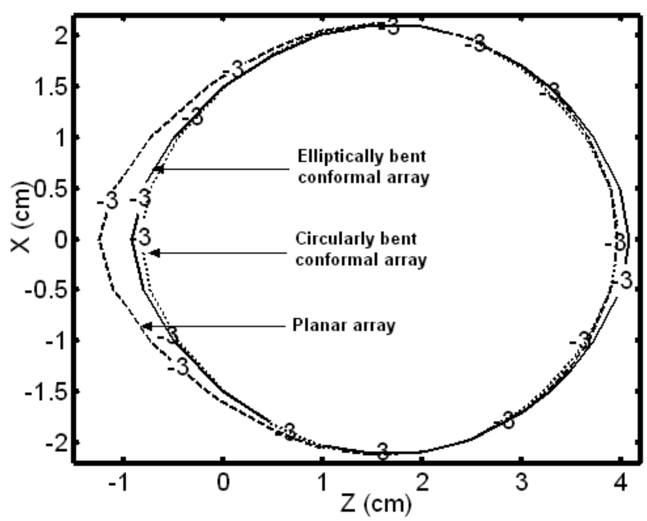

Figure 10. $-3\,\text{dB}$ SAR contour in x-z plane at $y = 3.5\,\text{cm}$ for phased arrays with different phase and amplitude excitation of each slot.

array under study is kept constant to observe the effect of amplitude excitation of each slot on the SAR distribution. The elliptically bent conformal phased array has larger EFS than other arrays (Table 1).

The -3 dB contour SAR distributions (in dB) in x-z plane for the profile of amplitude excitation given in Table 2 for each slot and for the phase calculated for each slot with the help of Eqn. (19) to focus at the point (0 cm, 3.5 cm, $z = 2$ cm) for elliptically and circularly bent conformal phased arrays and planar array are shown in Figure 10. In this case elliptically and circularly bent conformal arrays have almost identical focusing ability. Also conformal arrays have better focusing ability as compared with planar array.

3. CONCLUSION

The analysis approaches have been presented for SAR distributions in heating-medium (muscle/tumor) illuminated by a novel elliptically bent conformal array of longitudinal slots in narrow wall of water-loaded rectangular waveguide and the results for SAR distribution/contour have been compared with those for circular and planar arrays. It is shown that slotted conformal array can heat larger tumor area and has higher penetration depth in comparison to single slot applicator. It is shown that by adjusting phase and amplitude excitation of each slot, it is possible to heat tumors of arbitrary size selectively, *i.e.*, heating field size can controlled by adjusting phase and amplitude excitations of each slot. The present theory can be utilized to develop a novel, effective and realistic elliptically bent conformal array of longitudinal slots in narrow wall of water-loaded rectangular waveguide for hyperthermia treatment of cancer within the curved regions of human body, e.g., abdomen, neck, chest *etc.* The elliptically bent conformal phased array has better focusing ability under controlled amplitude and phase excitations of the elements as compared with planar array. Also, the elliptically bent conformal array confirms to the curved geometry of the human body in a better way as compared with other type of arrays considered.

ACKNOWLEDGMENT

Authors wish to thank the editorial board and reviewers for their invaluable suggestions to improve the quality of the paper. First author, Ramesh Chandra Gupta wishes to acknowledge to Department of Electronics Engineering, Institute of Technology-Banaras Hindu University (IT-BHU), Varanasi and University Grants Commission (UGC), New Delhi for awarding Senior Research Fellowship.

REFERENCES

1. Thuery, J., *Microwaves: Industrial, Scientific, and Medical Applications*, E. H. Grant (ed.), Artech House, 1992.
2. Gee, W., S.-W. Lee, N. K. Bong, C. A. Cain, R. Mittra, and R. L. Magin, "Focused array hyperthermia applicator: Theory and experiment," *IEEE Trans. Biomed. Eng.*, Vol. BME-31, No. 1, 38–46, Jan. 1984.
3. Castrillo, V. U., F. Chiadini, G. d'Ambrosio, V. Fiumara, R. Massa, G. Panariello, L. M. Pinto, and A. Scagione, "Waveguide slot applicators for microwave heating," *ICECom 2003, 17th Int. Conf. on Appl. EM and Comm.*, 49–51, Dubrovnik, Croatia, Oct. 1–3, 2003.
4. Hand, J. W., J. L. Cheetham, and A. J. Hand, "Absorbed power distributions from coherent microwave arrays for localized hyperthermia," *IEEE Trans. Microwave Theory Tech.*, Vol. MTT-34, No. 5, 484–489, May 1986.
5. Loane, J., H. Ling, B. F. Wang, and S. W. Lee, "Experimental investigation of a retro-focused microwave hyperthermia applicator: Conjugate-field matching scheme," *IEEE Trans. Microwave Theory Tech.*, Vol. MTT-34, No. 5, 490–494, May 1986.
6. Jouvie, F., J.-C. Bolomey, and G. Gaboriaaud, "Discussion of capabilities of microwave phased arrays for hyperthermia treatment of neck tumors," *IEEE Trans. Microwave Theory Tech.*, Vol. MTT-34, No. 5, 495–501, May 1986.
7. Paulides, M. M., S. H. J. A. Vossen, A. P. M. Zwamborn, and G. C. Van Roon, "Theoretical investigation into the feasibility to deposit RF energy centrally in the head-and-neck region," *Int. J. Radiation Oncology Biol. Phys.*, Vol. 63, No. 2, 634–642, 2005.
8. Wlodarczyk, W., J. Nadobny, P. Wust, G. Monich, P. Deuflhard, and R. Felix, "Systematic design of antennas for cylindrical 3D phased array hyperthermia applicator," *Proc. IEEE International Symposium Antennas and Propagation Society*, Vol. 2, 1004–1007, July 11–16, 1999.
9. Krairiksh, M., T. Wakabayashi, and W. Kiranon, "A spherical slot array applicator for medical applications," *IEEE Trans. Microwave Theory Tech.*, Vol. MTT-43, No. 1, 78–86, Jan. 1995.
10. Deng, T., "Optimization of SAR distributions in liver and lung regions irradiated by the H-horn annular phased array hyperthermia system," *IEEE Trans. Microwave Theory Tech.*, Vol. MTT-39, No. 5, 852–856, May 1991.
11. Wolff, E. A., *Antenna Analysis*, 139–192, Artech House, Norwood,

MA, 1988.

12. Silver, S. (ed.), *Microwave Antenna Theory and Design*, MIT Radiation Laboratory Series, Vol. 12, 123–135, 169–174, McGraw-Hill Book Company, New York, 1949.
13. Pandheripande, V. M. and B. N. Das, "Equivalent circuit of a narrow-wall waveguige slot coupler," *IEEE Trans. Microwave Theory Tech.*, Vol. MTT-27, No. 9, 800–804, Sept. 1979.
14. International Telephone and Telegraph Company, "Reference data for radio engineers," 5/e, H. W. Sams & Company Indianpolis, IN, 1968.
15. Schwan, H. P. and K. R. Foster, "RF field interactions with biological systems: Electrical properties and biophysical mechanism," *Proc. IEEE.*, Vol. 68, No. 1, 104–113, Jan. 1980.
16. Manson, P. A., W. D. Hurt, T. J. D'Andra, P. Gajšek, K. L. Ryan, D. A. Nelson, K. I. Smith, and J. M. Ziriax, "Effect of frequency, permittivity, and voxel size on predicted specific absorption rate values in biological tissue during electromagnetic field exposure," *IEEE Trans. Microwave Theory Tech.*, Vol. MTT-48, No. 1, 2050–2058, Jan. 2000.